

Fig. 4. Filament of an elongated target pattern. Both ends of the filament (solid line) terminate at the same boundary. If the filament obeys $N = D\kappa$, it will collapse in finite time. The lifetime of such an elongated target pattern is bounded above by the lifetime of the comparison curve (dashed line) consisting of a straight line with quarter-circular ends.

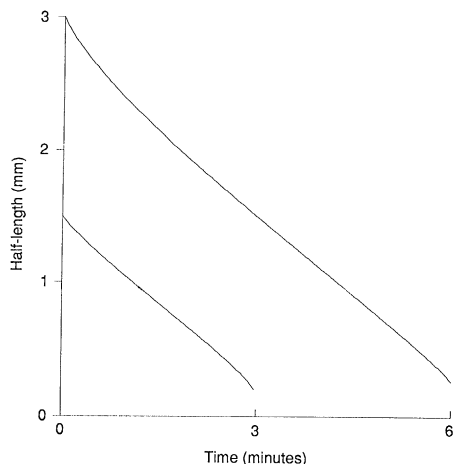


Fig. 5. Half-length of an elongated target pattern as a function of time. The equation of motion was solved numerically, starting with a semielliptical initial filament with maximal height 0.5 mm and initial half-lengths of 1.5 and 3 mm, with $D = 0.12 \text{ mm}^2/\text{min}$.

this curve initially will do so for all time. This is because the only point where the comparison curve moves with velocity equal to D times its curvature is at the end points and along the straight line. Everywhere else its normal velocity is less than D times its curvature. Thus if the end points are initially a distance x_0 apart, the time until collapse of the structure is $T_c < x_0 z_0 / 2D$.

This treatment suggests that elongated target patterns (hot dog sources) should shrink at a rate no slower than the constant rate $2D/z_0$. Numerical simulations confirm this estimate and show further that the collapse is nearly linear in time. Figure 5 shows the half-length as a function of time starting from a semielliptical filament with height 0.5 mm. For this filament the rate of collapse of the length was 0.81 mm/min compared with the estimate of 0.48 mm/min. From Winfree's time-lapse records of BZ waves, we measured the shortening of 11 hot dog sources and found that they did indeed shrink at a roughly constant rate (seven at 1 mm/min, three at 2 mm/min, and one at 0.5 mm/min).

Both hot dog sources and scroll rings have finite lifetimes, but hot dog sources disappear much more quickly than compar-

bly sized scroll rings. A hot dog source with initial length of 5 mm would have a lifetime of ~ 5 minutes, but a full scroll ring with the same initial diameter 5 mm would have a lifetime of ~ 26 minutes. Furthermore, the hot dog source shrinks linearly in time (for example, to half its initial length in 2.5 minutes), whereas a full scroll ring shrinks more slowly at first (for example, to half its initial diameter in 20 minutes). Thus the shrinking of hot dog sources should be much more noticeable than the shrinking of full scroll rings.

The equation of motion for an untwisted untorted scroll wave suggests that elongated spirals will evolve nearly exponentially into well-shaped (symmetric) spirals, whereas hot dog sources are unstable and will disappear in finite time. The time courses of these changes as predicted by the theory are in good agreement with experimental observations. The equation of motion $N = D\kappa$, therefore, gives a simple quantitative description of some features of scroll wave evolution. However, this equation of motion is incorrect in several respects. For one, it does not account for "drift" of scroll rings in a direction perpendicular to the plane of the ring (13, 16, 18). Furthermore, non-planar filaments have torsion and twist, but these variables are not accounted for by $N = D\kappa$. Third, it is observed numerically that under certain conditions scroll rings expand instead of shrink (18). This behavior is also inconsistent with the equation $N = D\kappa$, and has so far eluded theoretical understanding.

REFERENCES AND NOTES

1. A. T. Winfree, *Science* **175**, 634 (1972).
2. J. D. Gross, M. J. Peacey, D. J. Trevan, *J. Cell Sci.* **22**, 645 (1976); K. J. Tomchik and P. N. Devreotes, *Science* **212**, 443 (1981).
3. M. A. Allesie et al., *Circ. Res.* **333**, 54 (1973); A. T. Winfree, *Sci. Am.* **248**, 144 (May 1983).
4. V. I. Koroleva and J. Bures, *Brain Res.* **173**, 209 (1979); J. Bures, O. Buresova, V. I. Koroleva, in *Neurological Mechanisms of Epilepsy*, V. M. Okujava, Ed. (Metsniierba, Tbilisi, 1980), p. 120.
5. A. T. Winfree, *Science* **181**, 937 (1973).
6. ———, *Faraday Symp. Chem. Soc.* **9**, 38 (1975).
7. B. J. Welsh, J. Gomatam, A. E. Burgess, *Nature (London)* **304**, 611 (1983).
8. A. T. Winfree and S. H. Strogatz, *ibid.* **311**, 611 (1984).
9. A. T. Winfree, *Sci. Am.* **230**, 82 (June 1974).
10. A continuous space curve is described by a "moving trihedral" of three unit vectors, the tangent (T), normal (N), and binormal (B), which are functions of arc length (s) along the curve. By definition, curvature (κ) is $dT/ds \cdot N$ and torsion (τ) is $dB/ds \cdot N$. The twist $d\phi/ds$ of a scroll wave rotating around such a space curve is the change in phase (ϕ) with respect to arc length measured relative to the axes of the normal-binormal plane.
11. V. S. Zykov, *Biophysics* **25**, 906 (1980); *Modelling of Wave Processes in Excitable Media* (Manchester Univ. Press, Manchester, U.K., 1987).
12. J. P. Keener, *SIAM J. Appl. Math.* **46**, 1039 (1986); ——— and J. J. Tyson, *Physica* **21D**, 307 (1986).
13. A. V. Panfilov, A. N. Rudenko, V. I. Krinskii, *Biofizika* **31**, 850 (1986).
14. J. P. Keener, unpublished results.
15. K. A. Brakke, *Mathematical Notes* (Princeton Univ. Press, Princeton, NJ, 1978), vol. 20.
16. A. V. Panfilov and A. M. Pertsov, *Dokl. Biophys.* **274**, 58 (1984).
17. A. T. Winfree, unpublished photographs.
18. A. V. Panfilov and A. N. Rudenko, *Physica* **28D**, 215 (1987).
19. This work was supported in part by NSF grant DMS-8601134 (J.P.K.) and NSF grant MCS 83-01104 (J.J.T.). We thank A. T. Winfree who kindly made available to us his time-lapse photographs of scroll waves in BZ reagent.

25 September 1987; accepted 11 January 1988

A Cesium-Selective Ion Sieve Made by Topotactic Leaching of Phlogopite Mica

SRIDHAR KOMARNENI* AND RUSTUM ROY

A hydrated, sodium phlogopite mica with a c -axis spacing [$d(001)$] of 12.23 Å made by careful low-temperature leaching, showed extremely high selectivity for cesium. This newly discovered cesium ion sieve is useful in the decontamination as well as immobilization of cesium at room temperature through chemical bonding and may find applications in nuclear waste disposal and in decontamination of the environment after accidental releases of nuclear materials.

THE PRINCIPAL LONG-TERM PROBLEM caused by nuclear reactor accidents is the contamination of the environment with radioactive ^{137}Cs , as was evidenced by the Chernobyl nuclear reactor accident (1). This is because cesium is very volatile and can be carried long distances. Decontamination of the environment, humans, and animals is possible with the use of

a highly selective cesium ion sieve either by dispersion, for example, in water or soil, or by ingestion by humans and animals.

Zeolites and clay minerals are naturally occurring cation exchangers that have been

Materials Research Laboratory, Pennsylvania State University, University Park, PA 16802.

*To whom correspondence should be addressed.

used extensively in the decontamination and disposal of radioactive or nuclear wastes (2). The earliest waste disposal form that was developed for the immobilization of radioactive wastes was made with clay for use as a sponge for the uptake of different nuclides from waste water and its sintering (3). Much attention, however, has been directed toward the separation of radioactive ions such as ^{137}Cs by using zeolites, clay minerals, or synthetic cation exchangers (4) for decontamination or disposal (5). Mordenite has been used in Sweden in animal rations for decontamination from ^{137}Cs (5) which resulted from fallout of the Chernobyl nuclear reactor accident (1). The naturally occurring zeolite mordenite was suggested for the above purpose because it is more stable than the other zeolites under stomach acid conditions. The γ -phase of zirconium phosphate, $\gamma\text{-Zr}(\text{HPO}_4)_2 \cdot 2\text{H}_2\text{O}$, is an extremely selective cesium ion sieve (6) and we suggested that the γ -zirconium phosphate may be better suited for this purpose because of its much better resistance to acidity and much better selectivity for cesium (6). In fact, γ -zirconium phosphate can be prepared under acidic conditions near stomach pH (7). Thus inorganic cation exchangers

have been useful both in the decontamination and disposal of nuclear wastes. We report the discovery of a new cesium ion sieve that not only selectively exchanges cesium ions but also immobilizes them at room temperature through chemical bonding that also leads to the formation of a crystalline waste form at room temperature.

A naturally occurring phlogopite mica, $\text{KMg}_3\text{Si}_3\text{AlO}_{10}(\text{OH})_2$ (ideal formula) from near Perth, Ontario, was ground, and the particle fraction 0.2 to 20 μm in size was depleted of its potassium with sodium tetraphenylboron (NaTPB) by the method of Scott and Smith (8). The complete depletion of K^+ ions from the interlayers of the phlogopite mica and the simultaneous saturation of the interlayers with Na^+ ions along with a monolayer of water molecules by the above treatment resulted in a phase (K-depleted phlogopite mica) with a 12.23 Å c -axis (001) spacing, as opposed to the original phlogopite mica, which has a spacing of 10.03 Å (Fig. 1). The 12.23 Å phase [ideally $\text{NaMg}_3\text{Si}_3\text{AlO}_{10}(\text{OH})_2 \cdot \text{H}_2\text{O}$], that is, hydrated sodium phlogopite mica, was used in all of the following Cs^+ exchange experiments. We determined a Cs^+ exchange isotherm by equilibrating the K-depleted phlogopite mica in pure CsCl solutions containing 26.6 to 333 μg of cesium per milliliter for 4 days. The solid and solution phases were separated by centrifugation after equilibration. The solutions were analyzed for Cs^+ by atomic absorption spectroscopy (AAS), and the solid phase was characterized by powder x-ray diffraction (XRD). We investigated whether there was selective cesium exchange by determining a $\text{Na} \rightleftharpoons \text{Cs}$ exchange equilibrium with constant amounts of the K-depleted phlogopite mica, water, and total cations but with variable proportions of Cs^+ and Na^+ cations. The solid and solution phases were separated and analyzed as above after equilibration for 4 days. We also determined whether there was selective cesium uptake in the presence of a large excess of Na^+ or Ca^{2+} ($[\text{Na}^+]/[\text{Cs}^+]$ and $[\text{Ca}^{2+}]/[\text{Cs}^+]$ equivalent ratios are 200 and 100, respectively) by equilibrating 20 mg of K-depleted phlogopite mica for 1 day in 25 ml of 0.04M NaCl or 0.01M CaCl_2 containing 0.0002M CsCl . After equilibration the solid and solution phases were separated and analyzed as described above. The selective cesium uptake is expressed as K_d (in milliliters per gram) (9) values (K_d is a distribution coefficient defined as the ratio of the amount of cesium sorbed per gram of solid to the amount of cesium remaining per milliliter of solution). All of the data points represent the average of duplicate or triplicate runs with a mean variation of less than $\pm 2\%$.

Table 1. Comparative selective cesium-exchange behavior of K-depleted phlogopite mica and zeolites.

Sample	Cesium exchange, K_d (ml/g)	
	0.01M CaCl_2	0.04M NaNO_3
K-depleted phlogopite mica	664,000	949,000
γ -Zirconium phosphate	27,700	16,000
Mordenite, Nevada	165,000	4,300
Phillipsite, Nevada	34,500	9,800
Clinoptilolite, California	16,600	4,400

The cesium exchange isotherm of K-depleted phlogopite mica (Fig. 2) in the presence of pure CsCl solutions shows that a steady state was attained at a cesium loading of 93.7 meq/100 g in the presence of Na^+ released from the interlayers during equilibration. The K-depleted phlogopite mica has a theoretical exchange capacity of about 210 meq/100 g so that the cesium exchange that occurred was incomplete. This incomplete cesium exchange can be explained by the fact that the interlayer spacing significantly collapsed when about half of the exchange sites were occupied by cesium. Evidence for this collapse of interlayers was detected by powder XRD (Fig. 1C), which showed that the c -axis [$d(001)$] spacing decreased to 11.58 Å from 12.23 Å. The collapse of the interlayers can be explained by dehydration because of the high charge density of the layers and the low hydration energy of the cesium ions (10, 11). A closer examination of the XRD trace shows that a cesium mica (11) had formed, as revealed by the 10.65 Å c -axis spacing that can be derived from the $d(002)$, $d(003)$, and $d(004)$ spacings of 5.326, 3.557, and 2.661 Å, respectively. Indeed, the 10.65 Å c -axis spacing $d(001)$ appears as a shoulder on the 11.58 Å peak. The collapse of the c -axis spacing or the interlayer spacing by about 0.65 Å was effective in preventing any further exchange of Cs^+ ions from solution for Na^+ ions in the K-depleted phlogopite mica. Just as the cesium ions cannot enter the structure after the initial exchange, the cesium ions that entered the structure cannot escape from the collapsed interlayers, that is, effectively leading to the fixation of the cesium ions.

The equilibrium $\text{Na} \rightleftharpoons \text{Cs}$ exchange isotherm of K-depleted phlogopite mica is shown in Fig. 3. If the K-depleted phlogopite mica exhibits a preference for the entering cesium ion, the isotherm lies above the diagonal and vice versa (12). The diagonal line represents equal preference for both the ions. The cesium exchange isotherm falls

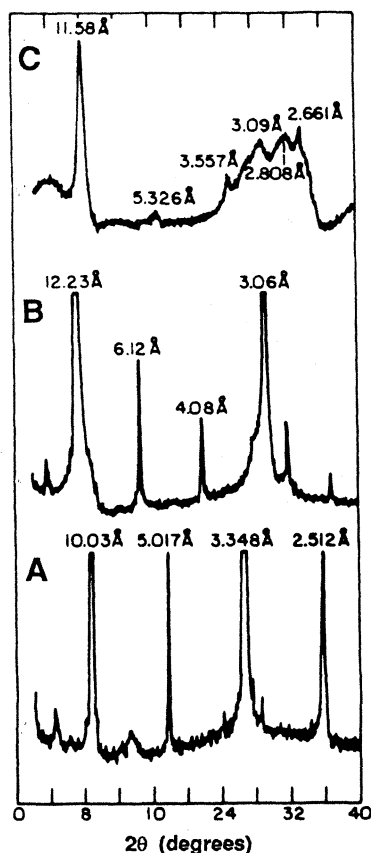


Fig. 1. X-ray diffraction traces ($\text{CuK}\alpha$ radiation): (A) untreated phlogopite mica, (B) K-depleted phlogopite mica, and (C) cesium-exchanged, K-depleted phlogopite mica.

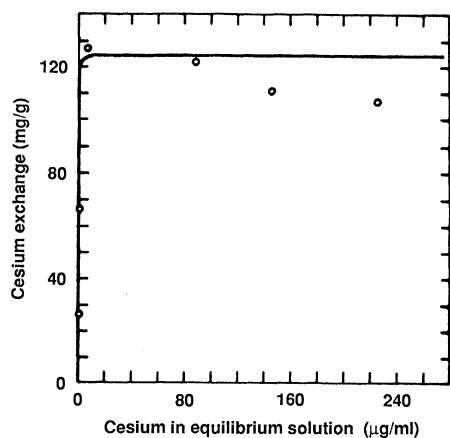


Fig. 2. Cesium exchange isotherm of K-depleted phlogopite mica with constant solid-solution ratio but increasing amounts of cesium.

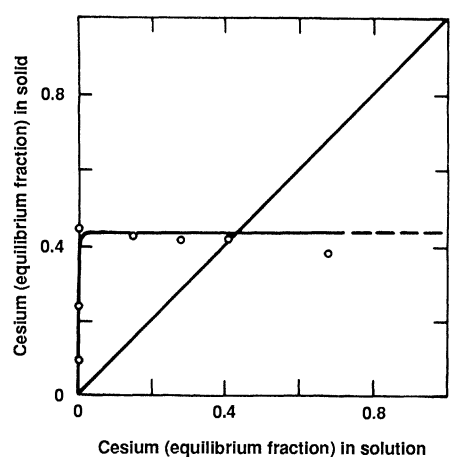


Fig. 3. Na ⇌ Cs exchange isotherm of K-depleted phlogopite mica with constant amounts of solid, water, and total cations, but variable proportions of Na⁺ and Cs⁺ cations.

above the diagonal line initially, which shows that Cs⁺ is highly preferred over Na⁺ initially. However, exchange does not go to completion, as indicated by the cesium exchange capacity of 91.4 meq/100 g, because of the interlayer collapsing and cesium ion trapping effect as described above. Cesium preference over sodium at the initial stages was extremely high, as indicated by the data points of the isotherm falling well above the diagonal line. The extreme preference of cesium over sodium ions in the K-depleted phlogopite mica is further attested by the fact that the total cesium exchange capacity is approximately the same whether sodium is present (91.4 meq of cesium per 100 g) or absent (93.7 meq of cesium per 100 g) in the equilibrating solution. The interlayer spacing of 2.89 Å is ideal for the diffusion of less hydrated cesium ions, just as in the case of γ -zirconium phosphate, which has an interlayer spacing of 2.85 Å (6).

A lower interlayer spacing would restrict the diffusion of all ions including cesium, whereas an increase in interlayer spacing

would allow much better access to other hydrated ions and thus limit the preference of cesium ions. The ideal interlayer spacing coupled with the high charge density of the layers is instrumental in the selective uptake and trapping of the cesium ions. Partially K-depleted biotite mica has been shown earlier to specifically exchange cesium (13), but fully K-depleted phlogopite mica has not been previously studied. Full potassium depletion results in a 12.23 Å *c*-axis *d*(001) spacing that is essential for obtaining the highest capacity and selectivity for cesium exchange.

The selectivity of the K-depleted phlogopite mica for cesium ions in the presence of excess Na⁺ and Ca²⁺ ions is compared with some of the cation exchangers that are presently used (Table 1). These results show that K-depleted phlogopite mica is by far the best material for selectively exchanging cesium from concentrated solutions containing Na⁺ or Ca²⁺, these two ions being dominant in natural waters.

REFERENCES AND NOTES

1. R. Wilson, *Science* **236**, 1636 (1987).
2. *Tech. Rep. Ser. No. 136* (International Atomic Energy Agency, Vienna, 1972), p. 61; *ibid.*, p. 64; M. W. Wilding and D. W. Rhodes, *U.S. At. Energy Comm.*

- Doc. No. IDO-14624* (1963); W. J. Lacy, *Ind. Eng. Chem.* **46**, 1061 (1954); T. Tamura, *Nucl. Eng. Design* **5**, 477 (1967).
3. J. M. Kerr, *Bull. Am. Ceram. Soc.* **38**, 374 (1954).
4. J. L. Nelson and B. W. Mercer, *U.S. At. Energy Comm. Doc. No. HW-76449* (1963); B. W. Mercer, L. L. Ames, P. W. Smith, *Nucl. Appl. Technol.* **8**, 62 (1970); T. Tamura and D. G. Jacobs, *Health Phys.* **2**, 391 (1960); B. L. Sawhney, *Soil Sci. Soc. Am. Proc.* **28**, 183 (1964); C. B. Amphlett, L. A. McDonald, M. J. Redman, *J. Inorg. Nucl. Chem.* **6**, 220 (1958); A. Clearfield and L. M. Jahangir, in *Recent Developments in Separation Science*, J. D. Navratil, Ed. (CRC Press, Boca Raton, FL, 1984), chap. 4; V. Vesely and V. Pekarek, *Talanta* **19**, 219 (1972).
5. S. Forberg, personal communication.
6. S. Komarneni and R. Roy, *Nature (London)* **299**, 707 (1982).
7. S. Yamanaka and M. Tanaka, *J. Inorg. Nucl. Chem.* **41**, 45 (1979).
8. A. D. Scott and S. J. Smith, *Clays Clay Miner.* **14**, 69 (1966).
9. T. Tamura, *Am. Assoc. Pet. Geol. Mem.* **18** (1972), pp. 318-330.
10. B. L. Sawhney, *Soil Sci. Soc. Am. Proc.* **33**, 42 (1969).
11. S. Komarneni and R. Roy, *Clay Miner.* **21**, 125 (1986).
12. D. W. Breck, *Zeolite Molecular Sieves, Structure, Chemistry, and Use* (Wiley, New York, 1974), p. 771.
13. T. Tamura, *U.S. At. Energy Comm. Rep. No. TID-7644* (1962), pp. 29-36; B. L. Sawhney, *Soil Sci. Soc. Am. Proc.* **31**, 181 (1967).
14. The authors acknowledge the financial support of the U.S. Department of Energy through the Division of Materials Science, Office of Basic Energy Sciences, under grant DE-FG02-85ER45204.

28 September 1987; accepted 22 January 1988

Generation of cDNA Probes Directed by Amino Acid Sequence: Cloning of Urate Oxidase

CHENG CHI LEE,* XIANGWEI WU, RICHARD A. GIBBS, RICHARD G. COOK, DONNA M. MUZNY, C. THOMAS CASKEY

Urate oxidase (E.C. 1.7.3.3) catalyzes the oxidation of uric acid to allantoin in most mammals except humans and certain primates. The amino-terminal amino acid sequence for porcine urate oxidase was determined and used in a novel procedure for generating complementary DNA (cDNA) probes to this amino acid sequence. The procedure is based on the polymerase chain reaction and utilizes mixed oligonucleotide primers complementary to the reverse translation products of an amino acid sequence. This rapid and simple cDNA cloning procedure is generally applicable and requires only a partial amino acid sequence. A cDNA probe developed by this procedure was used to isolate a full-length porcine urate oxidase cDNA and to demonstrate the presence of homologous genomic sequences in humans.

IN MOST MAMMALS, URATE OXIDASE IS present in the liver, with little or undetectable activity in other tissues. It is associated with the peroxisome and exists as a tetramer with an apparent subunit size of 32,000 daltons (1). Humans and certain primates lack this enzyme activity (2). Overproduction or elevated serum uric acid levels in man can lead to gouty arthritis. The recent identification of mice with complete hypoxanthine-guanine phosphoribosyl transferase (HPRT) deficiency that do

not display any of the symptoms of Lesch-Nyhan's syndrome has raised the possibility that the absence of urate oxidase activity in

C. C. Lee and R. A. Gibbs, Institute for Molecular Genetics, Baylor College of Medicine, Houston, TX 77030.

X. Wu, Department of Biochemistry, Baylor College of Medicine, Houston, TX 77030.

R. G. Cook, D. M. Muzny, C. T. Caskey, Howard Hughes Medical Institute, Baylor College of Medicine, Houston, TX 77030.

*To whom correspondence should be addressed.